



HAL
open science

Event-triggered output feedback control of traffic flow on cascaded roads

Nicolás Espitia, Jean Auriol, Huan Yu, Miroslav Krstic

► **To cite this version:**

Nicolás Espitia, Jean Auriol, Huan Yu, Miroslav Krstic. Event-triggered output feedback control of traffic flow on cascaded roads. *Advances in Distributed Parameter Systems*, pp 243-267, 2021, 978-3-030-94766-8. 10.1007/978-3-030-94766-8_11 . hal-03419923

HAL Id: hal-03419923

<https://hal.science/hal-03419923>

Submitted on 8 Nov 2021

HAL is a multi-disciplinary open access archive for the deposit and dissemination of scientific research documents, whether they are published or not. The documents may come from teaching and research institutions in France or abroad, or from public or private research centers.

L'archive ouverte pluridisciplinaire **HAL**, est destinée au dépôt et à la diffusion de documents scientifiques de niveau recherche, publiés ou non, émanant des établissements d'enseignement et de recherche français ou étrangers, des laboratoires publics ou privés.

Chapter 1

Event-triggered output feedback control of traffic flow on cascaded roads

Nicolas Espitia, Jean Auriol, Huan Yu, Miroslav Krstic

Abstract In this chapter, we develop an event-triggered boundary output feedback controller that guarantees the simultaneous stabilization of traffic flow on connected roads. The density and velocity traffic dynamics are described with the linearized Aw-Rascle-Zhang (ARZ) macroscopic traffic partial differential equation (PDE) model, which results in a coupled hyperbolic system. The control objective is to simultaneously stabilize the upstream and downstream traffic to a given spatially uniform constant steady-state that is in the congested regime. To suppress stop-and-go traffic oscillations on the cascaded roads, we consider a ramp metering strategy that regulates the traffic flow rate entering from the on-ramp to the mainline freeway. The ramp metering is located at the outlet with only boundary measurements of flow rate and velocity. The main idea is that the control signal is only updated when an event triggering condition is satisfied. Compared with the continuous input signal, the event-triggered boundary output control presents a more realistic setting to implement by ramp metering on a digital platform. The event-triggered boundary output control design relies on the emulation of the backstepping boundary output feedback and on a dynamic event-triggered

Nicolas Espitia

Univ. Lille, CNRS, Centrale Lille, UMR 9189 - CRISAL - Centre de Recherche en Informatique Signal et Automatique de Lille, F-59000 Lille, France. e-mail: nicolas.espitia-hoyos@univ-lille.fr

Jean Auriol

Université Paris-Saclay, CNRS, CentraleSupélec, Laboratoire des Signaux et Systèmes, 91190, Gif-sur-Yvette, France e-mail: jean.auriol@centralesupelec.fr

Huan Yu

Department of Mechanical and Aerospace Engineering, University of California, San Diego, La Jolla, CA 92093-0411, USA e-mail: huy015@eng.ucsd.edu

Miroslav Krstic

Department of Mechanical and Aerospace Engineering, University of California, San Diego, La Jolla, CA 92093-0411, USA e-mail: krstic@ucsd.edu

strategy to determine the time instants at which the control value must be updated. We prove that there is a uniform minimal dwell-time (independent of initial conditions), thus avoiding the so-called Zeno phenomenon. We guarantee the exponential convergence of the closed-loop system under the proposed event-triggered boundary control. A numerical example illustrates the results.

1.1 Introduction

Freeway traffic modeling and management have been intensively investigated due to the increasing demand of traffic mobility over the past decades. Various traffic control methods have been studied to regulate freeway traffic systems and mitigate traffic congestion. In particular, we focus on the stop-and-go traffic, a common phenomenon appearing on congested freeways. In congested traffic, drivers are forced into the acceleration-and-deceleration cycles. The stop-and-go traffic is characterized by such oscillations and causes increased consumption of fuel and unsafe driving conditions. We are interested in developing control strategies to mitigate stop-and-go oscillations.

Among different models for freeway traffic, macroscopic modeling is particularly suitable to describe the stop-and-go traffic since the propagation of traffic waves is described in the temporal and spatial domain. The macroscopic models predict the evolution of continuous traffic states by employing hyperbolic PDEs to govern traffic density and velocity dynamics. Among the models, the second-order Aw-Rascle-Zhang (ARZ) model [3] [20] for the stop-and-go traffic stands out. Indeed, the ARZ PDE model describes the traffic density and velocity of a freeway segment with two coupled hyperbolic PDEs. For more complex road network structures, the traffic network PDE model is developed in [9] [10] based on the family of ARZ models. Traffic control strategies are mainly developed and implemented on the traffic management infrastructures, that is, ramp metering and varying speed limits (VSL). Ramp metering controls the traffic lights on a ramp such that the inflow traffic is regulated for the mainline traffic. The VSL regulates traffic velocity by displaying driving velocities that are time-varying and dependent on real-time traffic. Boundary control algorithms have been developed for traffic control of a single freeway segment in [4] [12] [19] [21]. If we consider a traffic control problem on cascaded freeway segments, the application of these control laws needs to assume road homogeneity. In this chapter, we solve the the control problem of stop-and-go traffic congestion on cascaded freeway segments. We adopt the state-of-art second-order macroscopic traffic network models in [10], and we build on the linearized ARZ model around a steady-state in the congested regime. The model results in a coupled hyperbolic system with boundary input. We design the boundary control by the backstepping method and perform its emulation towards an event-triggered implementa-

tion. Hence, the boundary control signal is updated according to some policy while accounting for the information of estimated states (obtained from a suitable observer) and the error of the sampling scheduling. The triggering strategy, in turn, relies on a dynamic triggering condition which determines when the control action has to be updated. In this chapter, we only provide the results on avoidance of Zeno phenomenon, through the explicit characterization of a minimal inter-sampling time, and on the stability result for the closed-loop system under the event-triggered output control strategy.

1.2 Preliminaries and problem description

The evolution of traffic density $\rho_1(t, x)$ and velocity $v_1(t, x)$ (with $(t, x) \in [0, \infty) \times [0, L]$) on the downstream road segment and traffic density $\rho_2(t, s)$ and velocity $v_2(t, s)$ ($(t, s) \in [0, \infty) \times [-L, 0]$) on the upstream road segment are modeled by the following ARZ model.

$$\partial_t \rho_i + \partial_x (\rho_i v_i) = 0, \quad (1.1)$$

$$\partial_t (\rho_i (v_i + p_i)) + \partial_x (\rho_i v_i (v_i + p_i)) = -\frac{\rho_i (v_i - V_i(\rho_i))}{\tau_i}, \quad (1.2)$$

where $i \in \{1, 2\}$ represents downstream and upstream road respectively. The labeling of freeway segments is chosen as the reverse direction of traffic flow but same as the propagation direction of the control signal, which will be explained later. The traffic pressure $p_i(\rho_i)$ is defined as an increasing function of the density $p_i(\rho_i) = c_i \rho_i^{\gamma_i}$, where $\gamma_i, c_i \in \mathbb{R}^+ = [0, \infty)$ is defined as $c_i = v_m / \rho_{m,i}^{\gamma_i}$. The coefficient γ_i represents the overall drivers' property, reflecting their change of driving behavior to the increase of density. The changes in γ_i may reflect changes in the road properties (e.g. number of lanes). The positive constant v_m represents the maximum velocity and the positive constant $\rho_{m,i}$ is the maximum density defined as the number of vehicles per unit length. The equilibrium density-velocity relation $V_i(\rho_i)$ is given by $V_i(\rho_i) = v_m - p_i(\rho_i)$ for both segments, which assumes the same maximum velocity for the two segments when there are no vehicles on the road $\rho_i = 0$. We define the following variable

$$w_i = v_i + p_i(\rho_i), \quad (1.3)$$

which is interpreted as traffic "friction" or drivers' property [8]. This property transports in the traffic flow with vehicle velocity, representing the heterogeneity of individual driver with respect to the equilibrium density-velocity relation $V_i(\rho_i)$. The maximum velocity v_m is assumed to be the same for the two road segments while the maximum density $\rho_{m,i}$ and coefficient γ_i are allowed to vary. The positive constant τ_i is the relaxation time that represents the time scale for traffic velocity v_i adapting to the equilibrium density velocity relation $V_i(\rho_i)$. We denote the traffic flow rate on each road as $q_i = \rho_i v_i$

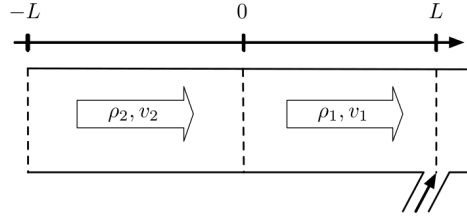


Fig. 1.1 Traffic flow on an incoming road and an outgoing road connected with a junction, actuation is implemented at the outlet with ramp metering.

The equilibrium flow and density relation, also known as the fundamental diagram, is then given by $Q_i(\rho_i) = \rho_i V(\rho_i) = \rho_i v_m (1 - (\rho_i / \rho_{m,i})^{\gamma_i})$. We assume that the equilibrium traffic relation is different for the two segments due to the change of road situations and access to road junction. The illustration is given in Fig 1.1. The critical density ρ_c segregates the free and congested regimes of traffic states. The critical density is given by $\rho_{c,i} = \rho_{m,i} / (1 + \gamma_i)^{1/\gamma_i}$ such that $Q'_i(\rho)|_{\rho=\rho_c} = 0$. The traffic is free when the density satisfies $\rho < \rho_{c,i}$. The traffic is defined as the congested one when the density satisfies $\rho > \rho_{c,i}$. For the free traffic, oscillations around the steady states will be damped out fast. For the congested traffic, there are two directional waves on road with one being the velocity oscillation propagating upstream and the other one being the density oscillation propagating downstream with the traffic. The congested traffic can become unstable [18]. We consider the situation that the upstream road segment 2 for $s \in [-L, 0]$ has more lanes than the downstream road segment for $x \in [0, L]$, in which congested traffic is usually formed up from downstream to upstream. Therefore, the maximum density $\rho_{m,2} > \rho_{m,1}$. The maximum driving speed v_m is assumed to be the same for the two segments. The maximum flow rate of the upstream road $Q_2(\rho_c)$ is reduced in the downstream to $Q_1(\rho_c)$, due to the change of road conditions from segment 2 to segment 1.

1.2.1 Actuated boundary

Regarding the boundary conditions connecting the two PDE systems, the Rankine-Hugoniot condition is satisfied at the junction such that the weak solution exists for the network (1.1)-(1.2) [14]. This condition implies piecewise smooth solutions and corresponds to the conservation of the mass and of the drivers' properties defined in (3) at the junction. Thus the flux and drivers' property are assumed to be continuous across the boundary conditions at $x = 0$, that is

$$\rho_1(t,0)v_1(t,0) = \rho_2(t,0)v_2(t,0), \quad (1.4)$$

$$w_2(t,0) = w_1(t,0). \quad (1.5)$$

For the open-loop system, we assume a constant inflow q^\star entering the inlet boundary $s = -L$ and a constant outflow q^\star at the outlet boundary for $x = L$:

$$q_2(t,-L) = q^\star \quad (1.6)$$

$$q_1(t,L) = q^\star \quad (1.7)$$

The control problem we solve consists of stabilizing on events the traffic flow in both the upstream and downstream road segments with a single actuator. Three possible locations for implementing a ramp metering control input are either at the inlet $x = -L$, at the junction $x = 0$ or at the outlet $x = L$ as in [17]. However, in this chapter we only present the observer-based event triggered control results for control input acting on the outlet and that is updated according to a suitable event-triggering condition. Note that the other cases could be solved adjusting the proposed techniques.

Ramp metering control $U_{\text{nom}}(t)$ from the outlet $x = L$: The downstream outflow at $x = L$ is actuated by $U_{\text{nom}}(t)$

$$q_1(t,L) = q^\star + U_{\text{nom}}(t), \quad (1.8)$$

where the outflow rate equals the summation of the onramp metering flow and the constant mainline flow. It should be noted that the designed controller U_{nom} is the flow rate perturbation around a nominal flow rate. We assume that the steady-state flow rate consists of a nominal onramp flow rate $q_r \geq 0$, which is a component of the steady-state flow rate q^\star . Then the actual ramp flow input at an onramp is given by

$$q_{\text{ramp}}(t) = q_r + U_{\text{nom}}(t) \geq 0. \quad (1.9)$$

In practice, we only need to guarantee that $q_{\text{ramp}}(t)$ is nonnegative so that $U_{\text{nom}}(t) \geq -q_r$. The value of q_r depends on the road configuration and real-time traffic conditions. We assume that there exists $q_r > 0$ such that (1.9) always holds. Combining the proposed control law with a saturation could guarantee that the proposed condition is satisfied.

1.2.2 Congested steady states

We are concerned with the congested traffic and assume that the equilibrium of both segments $(\rho_1^\star, v_1^\star), (\rho_2^\star, v_2^\star)$ are in the congested regime, which is the only one of theoretical control interest among all four traffic scenarios including free and free, free and congested, congested and free, congested and

congested. If the traffic of both segments is free, there is no need for ramp metering control. If the upstream segment 2 is in the free regime and the downstream segment 1 is congested, then we only need to control the congested downstream traffic with $U_{\text{nom}}(t)$ as presented in [19]. The oscillations propagated from the congested segment to the free regime segment will be damped out soon. The same applies to the scenario of free traffic in downstream segment 1 and congested traffic in upstream segment 2. The control objective is to stabilize the traffic flow in the two segments around the steady states. In practice, the steady states represent the equilibrium state values of the traffic flow when oscillations are successfully suppressed by our control design.

The steady states $(\rho_1^*, v_1^*), (\rho_2^*, v_2^*)$ are considered to be in the congested regime and the boundary conditions (1.4) and (1.5) are satisfied, i.e.,

$$\rho_1^* v_1^* = \rho_2^* v_2^* = q^*, \quad (1.10)$$

$$w_1^* = w_2^* = v_m, \quad (1.11)$$

where the steady state velocities satisfy the equilibrium density-velocity relation $v_i^* = V_i(\rho_i^*)$. According to (1.3) the constant driver's property in (1.11) implies that we have the same maximum velocity v_m for the two segments (which corresponds to our initial assumption):

$$v_1^* + p_1^* = v_2^* + p_2^* = v_m, \quad (1.12)$$

where $p_i^* = p_i(\rho_i^*)$. The steady states can be solved from the above nonlinear equations (1.10),(1.12) however there are no explicit solutions. Therefore we show the derivation process for obtaining the steady state values when ρ_1^* and the model parameters $v_m, \rho_{m,i}$ and γ_i are given. The functions $V_i(\rho)$, $Q_i(\rho)$ and $p_i(\rho)$ are also known. The steady state flow rate in (1.10) is obtained as $q^* = Q_1(\rho_1^*)$, and the constant flux $Q_1(\rho_1^*) = Q_2(\rho_2^*)$, yields a relation for the steady state densities of the two segments $\frac{\rho_1^* \rho_{m,1}^{\gamma_1} - (\rho_1^*)^{\gamma_1+1}}{\rho_2^* \rho_{m,2}^{\gamma_2} - (\rho_2^*)^{\gamma_2+1}} = \frac{\rho_{m,1}^{\gamma_1}}{\rho_{m,2}^{\gamma_2}}$. Knowing ρ_1^*, ρ_2^* and q^* , the steady states velocities are obtained as $v_i^* = q^* / \rho_i^*$.

1.2.3 Linearized ARZ model in Riemann coordinates

We linearize the ARZ based traffic network model (ρ_i, v_i) in (1.1),(1.2) with the boundary conditions (1.4),(1.5),(1.6),(1.7) around the steady states (ρ_i^*, v_i^*) defined in the previous section. In order to simplify the control design, the linearized model is then rewritten into the Riemann variables to which we apply an invertible spatial transformation

$$\bar{w}_i = \exp\left(\frac{x}{\tau_i v_i^*}\right) \left(\frac{\gamma_i p_i^*}{q^*} (\rho_i v_i - \rho_i^* v_i^*) + \frac{1}{r_i} (v_i - v_i^*) \right), \quad (1.13)$$

$$\bar{v}_i = v_i - v_i^*, \quad (1.14)$$

where $p_i^* = p_i(\rho_i^*)$ and the constant coefficients r_i are defined as

$$r_i = -\frac{v_i^*}{\gamma_i p_i^* - v_i^*}. \quad (1.15)$$

For the congested regime we have $\rho_i^* > \frac{\rho_{m,i}}{(1+\gamma_i)^{1/\gamma_i}}$ so that the characteristic speed $\gamma_i p_i^* - v_i^* > 0$. The velocity variations $\bar{v}_1(t, x)$ $\bar{v}_2(t, x)$ transport upstream which means the action of velocity acceleration or deceleration is repeated from the leading vehicle to the following vehicle. More precisely, we have $p_i^* = v_m - V(\rho_i^*) = v_m \left(\frac{\rho_i^*}{\rho_{m,i}}\right)^{\gamma_i} > v_m$, since $\rho_i^* > \frac{\rho_{m,i}}{(1+\gamma_i)^{1/\gamma_i}}$. Thus, $(\gamma_i + 2)p_i^* > 2v_m$, which implies $\gamma_i p_i^* > 2v_m - 2p_i^* = 2v_i^*$. Thus the inequalities $-1 < r_i < 0$ are satisfied for r_i defined in (1.15). The more congested the traffic, the lower the absolute value of this ratio. The linearized system with the controlled boundary condition (1.8) is written as

$$\partial_t \bar{w}_1(t, x) + v_1^* \partial_x \bar{w}_1(t, x) = 0, \quad (1.16)$$

$$\partial_t \bar{v}_1(t, x) - (\gamma_1 p_1^* - v_1^*) \partial_x \bar{v}_1(t, x) = \bar{c}_1(x) \bar{w}_1(t, x), \quad (1.17)$$

$$\partial_t \bar{w}_2(t, s) + v_2^* \partial_s \bar{w}_2(t, s) = 0, \quad (1.18)$$

$$\partial_t \bar{v}_2(t, s) - (\gamma_2 p_2^* - v_2^*) \partial_s \bar{v}_2(t, s) = \bar{c}_2(x) \bar{w}_2(t, s), \quad (1.19)$$

$$\bar{w}_1(t, 0) = \bar{w}_2(t, 0), \quad (1.20)$$

$$\bar{v}_1(t, L) = r_1 \exp\left(\frac{-L}{\tau_1 v_1^*}\right) \bar{w}_1(t, L) + \frac{1-r_1}{\rho_1^*} U_{\text{nom}}(t), \quad (1.21)$$

$$\bar{w}_2(t, -L) = \exp\left(\frac{-L}{\tau_2 v_2^*}\right) \frac{1}{r_2} \bar{v}_2(t, -L), \quad (1.22)$$

$$\bar{v}_2(t, 0) = \delta \frac{r_2}{r_1} \bar{v}_1(t, 0) + (1 - \delta) r_2 \bar{w}_2(t, 0), \quad (1.23)$$

where $s \in [-L, 0]$, $x \in [0, L]$, and where the spatially varying coefficient $\bar{c}_i(x)$ are defined by $\bar{c}_i(x) = -\frac{1}{\tau_i} \exp\left(-\frac{x}{\tau_i v_i^*}\right)$. The constant coefficient δ (ratio related to the traffic pressure of the segments) is defined by $\delta = \frac{\gamma_2 p_2^*}{\gamma_1 p_1^*}$. Although the cascade structure of the network presents some advantages for the design of a stabilizing control law (see [17]), it is more convenient for the design of an event-triggered algorithm to have all the states defined on the same spatial domain. The control diagram is shown in Fig. 1.2.

To rewrite the states \bar{w}_2 and \bar{v}_2 as functions defined on $[0, L]$, we consider the folding transformation $\bar{x} = -s$. The variable \bar{x} belongs to $[0, L]$. For sake of simplicity, we will omit the bar and abusively denote $\bar{w}_2(\bar{x}) = \bar{w}_2(x)$. With

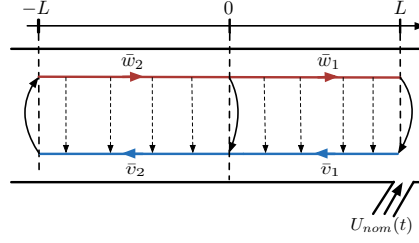


Fig. 1.2 Traffic flow on an incoming road and an outgoing road connected with a junction. Actuation is implemented at the outlet with ramp metering.

this transformation, the previous system rewrites

$$\partial_t \bar{w}_1(t, x) + v_1^* \partial_x \bar{w}_1(t, x) = 0, \quad (1.24)$$

$$\partial_t \bar{v}_1(t, x) - (\gamma_1 p_1^* - v_1^*) \partial_x \bar{v}_1(t, x) = c_1(x) \bar{w}_1(t, x), \quad (1.25)$$

$$\partial_t \bar{w}_2(t, x) - v_2^* \partial_x \bar{w}_2(t, x) = 0, \quad (1.26)$$

$$\partial_t \bar{v}_2(t, x) + (\gamma_2 p_2^* - v_2^*) \partial_x \bar{v}_2(t, x) = c_2(x) \bar{w}_2(t, x), \quad (1.27)$$

$$\bar{w}_1(t, 0) = \bar{w}_2(t, 0), \quad (1.28)$$

$$\bar{v}_1(t, L) = r_1 \exp\left(\frac{-L}{\tau_1 v_1^*}\right) \bar{w}_1(t, L) + \frac{1-r_1}{\rho_1^*} U_{\text{nom}}(t), \quad (1.29)$$

$$\bar{w}_2(t, L) = \exp\left(\frac{-L}{\tau_2 v_2^*}\right) \frac{1}{r_2} \bar{v}_2(t, L), \quad (1.30)$$

$$\bar{v}_2(t, 0) = \delta \frac{r_2}{r_1} \bar{v}_1(t, 0) + (1 - \delta) r_2 \bar{w}_2(t, 0), \quad (1.31)$$

where $x \in [0, L]$, and $c_1(x) = \bar{c}_1(x)$ and $c_2(x) = \bar{c}_2(-x)$. The open-loop system (1.24)-(1.31) (for which $U_{\text{nom}} \equiv 0$) is well-posed in the sense of the L^2 norm (weak solutions) by [4, Theorem A.4], that is, for any initial conditions $(\bar{v}_0)_i, (\bar{w}_0)_i \in (L^2([0, L]))^2$, there is only one L^2 -solution. It is shown in [19] that only marginal linear stability holds for the open-loop system of one segment. The control operator is admissible (i.e. it verifies the so-called admissibility condition as stated in [11]). Consequently, for any $U_L \in L^2([0, T])$, and for any initial conditions $(\bar{v}_0)_i, (\bar{w}_0)_i \in (L^2([0, L]))^2$ there is only one L^2 -solution to (1.24)-(1.31). We assume that the available measurement corresponds to the values of \bar{q}_i and \bar{v}_i at the left side of the outlet $x = L$. Since $\bar{w}_1(t, L) = \exp\left(\frac{-L}{\tau_1 v_1^*}\right) \left(\frac{\gamma_1 p_1^*}{q^*} \bar{q}_1(t, L) - \frac{1}{r_1} \bar{v}_1(t, L)\right)$, we can consider that

$$Y_L(t) = \bar{w}_1(t, L). \quad (1.32)$$

We make the following non-restrictive assumption so that the proposed feedback laws have some (delay)-robustness margins.

Assumption The boundary couplings of the system (1.24)-(1.31) are such that

$$\delta < \frac{1+\exp(\frac{L}{\tau_2 v_2^*})}{1+\exp(\frac{-L}{\tau_1 v_1^*})} \quad \text{if } \delta > 1, \quad \delta < \frac{1-\exp(\frac{L}{\tau_2 v_2^*})}{1-\exp(\frac{-L}{\tau_1 v_1^*})} \quad \text{if } \delta \leq 1, \quad (1.33)$$

If this assumption is not satisfied, then it is not possible to robustly stabilize the system (1.24)-(1.31) when there are input delays (as the open-loop transfer function would have an infinite chain of poles in the complex right half-plane) see [17] and [1] for details. Moreover, it can be shown (see [1]) that this condition implies that the system (1.24)-(1.31) is exponentially stable in the absence of in-domain couplings and actuation. Thus, this assumption means that in the absence of in-domain couplings, the system is naturally dissipative.

The control objective is to simultaneously stabilize the upstream and downstream traffic to a given spatially uniform constant steady-state. We propose an output feedback controller located at the outlet of the downstream traffic with collocated sensing of flow rate and velocity at the outlet. The state feedback and observer designs are based on the PDE backstepping methodology. The exponential stability in the sense of L^2 -norm of the under-actuated network of two systems of two hyperbolic PDEs is guaranteed. Considering the continuous boundary control and estimation designs need to be implemented into digital platforms, we develop event-triggered boundary controllers which stabilize the system on events. The proposed event-triggered controllers are piecewise constant, and the control value is updated based on a dynamic triggering condition only when needed i.e. once a given deviation term (that will be defined below) becomes larger than a Lyapunov functional.

1.3 Output-feedback stabilization and emulation of the control law

An output-feedback law $U_{\text{nom}}(t)$ has been proposed in [17] to stabilize the system (1.24)-(1.31). Here, we aim at stabilizing the closed-loop system (1.24)-(1.31) on events while updating the continuous-time controller $U_{\text{nom}}(t)$ at certain sequence of time instants $(t_k)_{k \in \mathbb{N}}$, that will be characterized later on. The control value is held constant between two successive time instants and it is updated when some triggering condition is verified. This procedure is referred to as *event-triggering*. It is an efficient way to suitably sample the control value, thus avoiding useless actuation solicitations. To that end, we need to modify the control law proposed in [17]. More precisely, the control law $U_{\text{nom}}(t)$ will be replaced by $U_{\text{nom}}(t_k)$ for all $t \in [t_k, t_{k+1})$, $k \geq 0$. Consequently, we have $U_{\text{nom}}(t_k) = U_{\text{nom}}(t) + d(t)$, where d can be seen as a deviation of actuation. In what follows, we recall the observer/controller

design proposed in [17] using the backstepping transformations since these transformations will be crucial to prove that our emulated control law still stabilizes the system (1.24)-(1.31). We define the sets $\bar{\mathcal{T}}_1, \bar{\mathcal{T}}_2$ as follows

$$\bar{\mathcal{T}}_1 = \{(x, \xi) \in [0, L]^2, \xi \geq x\}, \quad \bar{\mathcal{T}}_2 = \{(x, \xi) \in [0, L]^2, \xi \leq x\}. \quad (1.34)$$

Finally, the set $\bar{\mathcal{T}}_3$ is defined as the unit square $[0, L]^2$: $\bar{\mathcal{T}}_3 = \{(x, \xi) \in [0, L]^2\}$. The set $\bar{\mathcal{T}}_1$ is the upper-part of this square while $\bar{\mathcal{T}}_2$ corresponds to its lower part.

1.3.1 Observer design

The first step for the design of an output-feedback law is the design of a state estimator. Consider an arbitrary control law $U_{\text{nom}}(t_k)$ acting on the system (1.24)-(1.31), for all $t \in [t_k, t_{k+1})$. We will defined \hat{w}_i and \hat{v}_i as the observer states. The error states are defined as the difference between the real states and their estimations: $\tilde{w}_i = \bar{w}_i - \hat{w}_i$ and $\tilde{v}_i = \bar{v}_i - \hat{v}_i$. A suitable observer system is defined in [17] by

$$\partial_t \hat{w}_1(t, x) + v_1^* \partial_x \hat{w}_1(t, x) = -\mu_1(x) \tilde{w}_1(t, L), \quad (1.35)$$

$$\partial_t \hat{v}_1(t, x) - (\gamma_1 p_1^* - v_1^*) \partial_x \hat{v}_1(t, x) = c_1(x) \hat{w}_1(t, x) - v_1(x) \tilde{w}_1(t, L), \quad (1.36)$$

$$\partial_t \hat{w}_2(t, x) - v_2^* \partial_x \hat{w}_2(t, x) = -\mu_2(x) \tilde{w}_1(t, L), \quad (1.37)$$

$$\partial_t \hat{v}_2(t, x) + (\gamma_2 p_2^* - v_2^*) \partial_x \hat{v}_2(t, x) = c_2(x) \tilde{w}_2(t, x) - v_2(x) \tilde{w}_1(t, L), \quad (1.38)$$

$$\hat{w}_1(t, 0) = \hat{w}_2(t, 0), \quad (1.39)$$

$$\hat{v}_1(t, L) = r_1 \exp\left(\frac{-L}{\tau_1 v_1^*}\right) \hat{w}_1(t, L) + \frac{1-r_1}{\rho_1^*} U_{\text{nom}}(t_k), \quad (1.40)$$

$$\hat{w}_2(t, L) = \exp\left(\frac{-L}{\tau_2 v_2^*}\right) \frac{1}{r_2} \hat{v}_2(t, L), \quad (1.41)$$

$$\hat{v}_2(t, 0) = \delta \frac{r_2}{r_1} \hat{v}_1(t, 0) + (1 - \delta) r_2 \hat{w}_2(t, 0), \quad (1.42)$$

where \hat{w}_i, \hat{v}_i are the estimates of the state variables \bar{w}_i, \bar{v}_i in (1.24)-(1.31). The corresponding initial conditions are L^2 functions. The terms μ_i and v_i are the output injection terms that are given as follows [17]:

$$\mu_1(x) = v_1^* N_1^{\alpha\alpha}(x, L), \quad v_1(x) = v_1^* N_1^{\beta\alpha}(x, L), \quad (1.43)$$

$$\mu_2(x) = v_1^* N^{\alpha}(x, L), \quad v_2(x) = v_1^* N^{\beta}(x, L), \quad (1.44)$$

where the kernels $N_1^{\alpha\alpha}, N_1^{\alpha\beta}$ are bounded functions defined on $\bar{\mathcal{T}}_1$, the kernels $N_2^{\alpha\alpha}, N_2^{\alpha\beta}$ are bounded functions defined on $\bar{\mathcal{T}}_2$, and the kernels N^{α}, N^{β} are bounded functions defined on $\bar{\mathcal{T}}_3$. They satisfy the following set of equations

for all (x, ξ) that belong to their respective domain of definition

$$\partial_x N_i^{\alpha\alpha}(x, \xi) + \partial_\xi N_i^{\alpha\alpha}(x, \xi) = 0, \quad (1.45)$$

$$(\gamma_1 p_1^* - v_1^*) \partial_x N_1^{\beta\alpha}(x, \xi) - v_1^* \partial_\xi N_1^{\beta\alpha}(x, \xi) = -c_1(x) N_1^{\alpha\alpha}(x, \xi), \quad (1.46)$$

$$(\gamma_2 p_2^* - v_2^*) \partial_x N_2^{\beta\alpha}(x, \xi) - v_2^* \partial_\xi N_2^{\beta\alpha}(x, \xi) = c_2(x) N_2^{\alpha\alpha}(x, \xi), \quad (1.47)$$

$$v_2^* \partial_x N^\alpha(x, \xi) - v_1^* \partial_\xi N^\alpha(x, \xi) = 0, \quad (1.48)$$

$$(\gamma_2 p_2^* - v_2^*) \partial_x N^\beta(x, \xi) + v_1^* \partial_\xi N^\beta(x, \xi) = c_2(x) N^\alpha(x, \xi), \quad (1.49)$$

with the boundary conditions

$$N_i^{\beta\alpha}(x, x) = -\frac{c_i(x)}{\gamma_i p_i^*}, \quad N_1^{\alpha\alpha}(0, \xi) = N^\alpha(0, \xi), \quad N^\beta(x, 0) = \frac{v_2^*}{v_1^*} N_2^{\beta\alpha}(x, 0) \quad (1.50)$$

$$N^\alpha(x, 0) = \frac{v_2^*}{v_1^*} N_2^{\alpha\alpha}(x, 0), \quad N^\beta(0, \xi) = \delta \frac{r_2}{r_1} N_1^{\beta\alpha}(0, \xi) + (1 - \delta) r_2 N^\alpha(0, \xi), \quad (1.51)$$

$$N^\alpha(L, \xi) = \exp\left(-\frac{L}{\tau_2 v_2^*}\right) \frac{1}{r_2} N^\beta(L, \xi), \quad N_2^{\alpha\alpha}(L, \xi) = \exp\left(-\frac{L}{\tau_2 v_2^*}\right) \frac{1}{r_2} N_2^{\beta\alpha}(L, \xi). \quad (1.52)$$

Equations (1.45)-(1.52) admit a unique solution, as proved in [17]. It has been shown in [17] that such an observer guarantees the convergence of the estimated states to the real states, that is the error states converge to zero. The error system (that will be useful to design our event-triggered control law) rewrites as

$$\partial_t \tilde{w}_1(t, x) + v_1^* \partial_x \tilde{w}_1(t, x) = \mu_1(x) \tilde{w}_1(t, L), \quad (1.53)$$

$$\partial_t \tilde{v}_1(t, x) - (\gamma_1 p_1^* - v_1^*) \partial_x \tilde{v}_1(t, x) = c_1(x) \tilde{w}_1(t, x) + v_1(x) \tilde{w}_1(t, L), \quad (1.54)$$

$$\partial_t \tilde{w}_2(t, x) - v_2^* \partial_x \tilde{w}_2(t, x) = \mu_2(x) \tilde{w}_1(t, L), \quad (1.55)$$

$$\partial_t \tilde{v}_2(t, x) + (\gamma_2 p_2^* - v_2^*) \partial_x \tilde{v}_2(t, x) = c_2(x) \tilde{w}_2(t, x) + v_2(x) \tilde{w}_1(t, L), \quad (1.56)$$

$$\tilde{w}_1(t, 0) = \tilde{w}_2(t, 0), \quad (1.57)$$

$$\tilde{v}_1(t, L) = r_1 \exp\left(\frac{-L}{\tau_1 v_1^*}\right) \tilde{w}_1(t, L), \quad (1.58)$$

$$\tilde{w}_2(t, L) = \exp\left(\frac{-L}{\tau_2 v_2^*}\right) \frac{1}{r_2} \tilde{v}_2(t, L), \quad (1.59)$$

$$\tilde{v}_2(t, 0) = \delta \frac{r_2}{r_1} \tilde{v}_1(t, 0) + (1 - \delta) r_2 \tilde{w}_2(0) \quad (1.60)$$

To show that this error system is exponentially stable, we shall consider the following backstepping transformation

$$\begin{aligned}
\begin{pmatrix} \tilde{w}_1(t,x) \\ \tilde{v}_1(t,x) \\ \tilde{w}_2(t,x) \\ \tilde{v}_2(t,x) \end{pmatrix} &:= \mathcal{N} \begin{pmatrix} \tilde{\alpha}_1(t,x) \\ \tilde{\beta}_1(t,x) \\ \tilde{\alpha}_2(t,x) \\ \tilde{\beta}_2(t,x) \end{pmatrix} (x) \\
&= \begin{pmatrix} \tilde{\alpha}_1(t,x) \\ \tilde{\beta}_1(t,x) \\ \tilde{\alpha}_2(t,x) \\ \tilde{\beta}_2(t,x) \end{pmatrix} - \int_0^L \begin{pmatrix} N_1^{\alpha\alpha}(x,\xi)\mathbb{1}_{[x,L]}(\xi) & 0 & 0 \\ N_1^{\beta\alpha}(x,\xi)\mathbb{1}_{[x,L]}(\xi) & 0 & 0 \\ N^\alpha(x,\xi) & 0 & N_2^{\alpha\alpha}(x,\xi)\mathbb{1}_{[0,x]}(\xi) \\ N^\beta(x,\xi) & 0 & N_2^{\beta\alpha}(x,\xi)\mathbb{1}_{[0,x]}(\xi) \end{pmatrix} \begin{pmatrix} \tilde{\alpha}_1(t,\xi) \\ \tilde{\beta}_1(t,\xi) \\ \tilde{\alpha}_2(t,\xi) \\ \tilde{\beta}_2(t,\xi) \end{pmatrix} d\xi.
\end{aligned} \tag{1.61}$$

where the different kernels are defined by (1.45)-(1.52). The transformation (1.61) is invertible. This can be seen, noticing first that the part acting on the states $\tilde{\alpha}_1$ and $\tilde{\beta}_1$ corresponds to a Volterra transformation (which is always invertible [16]). Then, the part acting on the states $\tilde{\alpha}_2$ and $\tilde{\beta}_2$ corresponds to Volterra transformation to which is added an affine term that depends on $\tilde{\alpha}_1$ and $\tilde{\beta}_1$. This transformation, maps the error system (1.53)-(1.60) to the system

$$\partial_t \tilde{\alpha}_i(t,x) + v_i^* \partial_x \tilde{\alpha}_i(t,x) = 0, \tag{1.62}$$

$$\partial_t \tilde{\beta}_i(t,x) - (\gamma_i p_i^* - v_i^*) \partial_x \tilde{\beta}_i(t,x) = 0, \tag{1.63}$$

$$\tilde{\alpha}_1(t,0) = \tilde{\alpha}_2(t,0), \tag{1.64}$$

$$\tilde{\beta}_1(t,L) = r_1 \exp\left(\frac{-L}{\tau_1 v_1^*}\right) \tilde{\alpha}_1(t,L), \tag{1.65}$$

$$\tilde{\alpha}_2(t,L) = \exp\left(\frac{-L}{\tau_2 v_2^*}\right) \frac{1}{r_2} \tilde{\beta}_2(t,L), \tag{1.66}$$

$$\tilde{\beta}_2(t,0) = \delta \frac{r_2}{r_1} \tilde{\beta}_1(t,0) + (1-\delta)r_2 \tilde{\alpha}_2(0), \tag{1.67}$$

This target system is exponentially stable due to Assumption 1. The design of our event-triggered procedure requires, the inverse transformation of (1.61). More precisely, we denote \mathcal{R} the corresponding inverse transformation. It satisfies

$$\begin{aligned}
\begin{pmatrix} \tilde{\alpha}_1(t,x) \\ \tilde{\beta}_1(t,x) \\ \tilde{\alpha}_2(t,x) \\ \tilde{\beta}_2(t,x) \end{pmatrix} &:= \mathcal{R} \begin{pmatrix} \tilde{w}_1(t,\cdot) \\ \tilde{v}_1(t,\cdot) \\ \tilde{w}_2(t,\cdot) \\ \tilde{v}_2(t,\cdot) \end{pmatrix} (x) \\
&= \begin{pmatrix} \tilde{w}_1(t,x) \\ \tilde{v}_1(t,x) \\ \tilde{w}_2(t,x) \\ \tilde{v}_2(t,x) \end{pmatrix} - \int_0^L \begin{pmatrix} R_1^{wv}(x,\xi)\mathbb{1}_{[x,L]}(x) & 0 & 0 \\ R_1^{vw}(x,\xi)\mathbb{1}_{[x,L]}(x) & 0 & 0 \\ R^w(x,\xi) & 0 & R_2^{wv}(x,\xi)\mathbb{1}_{[0,x]}(x) \\ R^v(x,\xi) & 0 & R_2^{vv}(x,\xi)\mathbb{1}_{[0,x]}(x) \end{pmatrix} \begin{pmatrix} \tilde{w}_1(t,\xi) \\ \tilde{v}_1(t,\xi) \\ \tilde{w}_2(t,\xi) \\ \tilde{v}_2(t,\xi) \end{pmatrix} d\xi
\end{aligned} \tag{1.68}$$

Again, the different kernels are bounded functions defined on $\bar{\mathcal{T}}_1$ (kernels R_1^{\cdot}), $\bar{\mathcal{T}}_2$ (kernels R_2^{\cdot}) or $\bar{\mathcal{T}}_3$ (kernels R^{\cdot}). They satisfy the following set of equations on their respective domain of definition

$$\partial_x R_i^{ww}(x, \xi) + \partial_\xi R_i^{ww}(x, \xi) = 0, \quad (1.69)$$

$$(\gamma_i p_i^* - v_i^*) \partial_x R_i^{vw}(x, \xi) - v_i^* \partial_\xi R_i^{vw}(x, \xi) = 0, \quad (1.70)$$

$$v_2^* \partial_x R^w(x, \xi) - v_1^* \partial_\xi R^w(x, \xi) = 0, \quad (1.71)$$

$$(\gamma_2 p_2^* - v_2^*) \partial_x R^v(x, \xi) + v_2^* \partial_\xi R^v(x, \xi) = 0, \quad (1.72)$$

with the boundary conditions

$$R_i^{vw}(x, x) = \frac{c_i(x)}{\gamma_i p_i^*}, \quad R_1^{ww}(0, \xi) = R^w(0, \xi), \quad (1.73)$$

$$R^w(x, 0) = \frac{v_2^*}{v_1^*} R_2^{ww}(x, 0), \quad R^v(x, 0) = \frac{v_2^*}{v_1^*} R_2^{vw}(x, 0), \quad (1.74)$$

$$R^v(0, \xi) = \delta \frac{r_2}{r_1} R_1^{vw}(0, \xi) + (1 - \delta) r_2 R^w(0, \xi), \quad (1.75)$$

$$R^w(L, \xi) = \exp\left(-\frac{L}{\tau_2 v_2^*}\right) \frac{1}{r_2} R^v(L, \xi), \quad (1.76)$$

$$R_2^{ww}(L, \xi) = \exp\left(-\frac{L}{\tau_2 v_2^*}\right) \frac{1}{r_2} R_2^{vw}(L, \xi), \quad (1.77)$$

1.3.2 Output feedback control law (nominal)

Using the proposed observer, we can now design an output-feedback control law. More precisely, the following control law has been proposed in [17]

$$U_{\text{nom}}(t) = \frac{\rho_1^*}{1-r_1} \left(\int_0^L K_1^{vw}(L, \xi) \hat{w}_1(\xi, t) d\xi + K_1^{vv}(L, \xi) \hat{v}_1(\xi, t) d\xi \right. \\ \left. + \int_0^L K^w(L, \xi) \hat{w}_2(\xi, t) d\xi \int_0^L K^v(L, \xi) \hat{v}_2(\xi, t) d\xi \right), \quad (1.78)$$

where the kernels K_1^{vw} and K_1^{vv} that are bounded functions defined on $\bar{\mathcal{T}}_2$, the kernels K_2^{vw} and K_2^{vv} are bounded functions defined on $\bar{\mathcal{T}}_1$, and the kernels K^w and K^v that are bounded functions defined on $\bar{\mathcal{T}}_3$. On their corresponding domain of definition, they verify

$$(\gamma_1 p_1^* - v_1^*) \partial_x K_1^{vw}(x, \xi) - v_1^* \partial_\xi K_1^{vw}(x, \xi) = c_1(\xi) K_1^{vv}(x, \xi), \quad (1.79)$$

$$(\gamma_2 p_2^* - v_2^*) \partial_x K_2^{vw}(x, \xi) - v_2^* \partial_\xi K_2^{vw}(x, \xi) = -c_2(\xi) K_2^{vv}(x, \xi) \quad (1.80)$$

$$\partial_x K_i^{vv}(x, \xi) + \partial_\xi K_i^{vv}(x, \xi) = 0, \quad (1.81)$$

$$(\gamma_1 p_1^* - v_1^*) \partial_x K^v(x, \xi) - (\gamma_2 p_2^* - v_2^*) \partial_\xi K^v(x, \xi) = 0, \quad (1.82)$$

$$(\gamma_1 p_1^* - v_1^*) \partial_x K^w(x, \xi) + v_2^* \partial_\xi K^w(x, \xi) = c_2(\xi) K^v(x, \xi), \quad (1.83)$$

with the boundary conditions

$$K_i^{vw}(x, x) = -\frac{c_i(x)}{\gamma_i p_i^*}, K_1^{vv}(x, 0) = \frac{v_2^*}{v_1^*} \delta K^v(x, 0), \quad (1.84)$$

$$K^v(0, \xi) = \frac{r_1}{\delta r_2} K_2^{vv}(0, \xi), K^v(x, L) = -\exp\left(\frac{-L}{\tau_2 v_2^*}\right) K^w(x, L), \quad (1.85)$$

$$K_2^{vv}(x, L) = -\exp\left(\frac{-L}{\tau_2 v_2^*}\right) K_2^{vw}(x, L), K^w(0, \xi) = \frac{r_1}{\delta r_2} K_2^{vw}(0, \xi), \quad (1.86)$$

$$K^w(x, 0) = -(1 - \delta)K^v(x, 0) + \frac{v_1^*}{v_2^*} K_1^{vw}(x, 0). \quad (1.87)$$

It has been shown in [17] that the kernels equations (1.79)-(1.87) admit a unique solution. Since the kernels are bounded functions, our control operator is a linear bounded operator, and the control law U_{nom} is continuous. It is also strictly proper as it is only composed of integral terms. The exponential stability of the closed-loop system has been shown in [17]. Following the ideas of [2], we can prove that it is robust with respect to delays in the actuation and uncertainties on the parameters. For practical implementation of the ramp metering control input, we need to modulate the changing frequency of the on-ramp traffic light. This is one additional motivation for using an event-triggered procedure which is a way to implement the continuous-time controllers into digital forms by updating the input values only when needed. To show that the closed-loop system (1.24)-(1.31) with the control law (1.78) is exponentially stable in the sense of the L^2 norm, we can use the backstepping transformation

$$\begin{aligned} \begin{pmatrix} \hat{\alpha}_1(t, x) \\ \hat{\beta}_1(t, x) \\ \hat{\alpha}_2(t, x) \\ \hat{\beta}_2(t, x) \end{pmatrix} &:= \left(\mathcal{K} \begin{pmatrix} \hat{w}_1(t, \cdot) \\ \hat{v}_1(t, \cdot) \\ \hat{w}_2(t, \cdot) \\ \hat{v}_2(t, \cdot) \end{pmatrix} \right) (x) \\ &= \begin{pmatrix} \hat{w}_1(t, \cdot) \\ \hat{v}_1(t, \cdot) \\ \hat{w}_2(t, \cdot) \\ \hat{v}_2(t, \cdot) \end{pmatrix} - \int_0^L \begin{pmatrix} 0 & K_1^{vw}(x, \xi) \mathbb{1}_{[0, x]}(\xi) & 0 & 0 \\ 0 & K_1^{vv}(x, \xi) \mathbb{1}_{[0, x]}(\xi) & 0 & 0 \\ 0 & K^w(x, \xi) & 0 & K_2^{vw}(x, \xi) \mathbb{1}_{[x, L]}(\xi) \\ 0 & K^v(x, \xi) & 0 & K_2^{vv}(x, \xi) \mathbb{1}_{[x, L]}(\xi) \end{pmatrix}^T \begin{pmatrix} \hat{w}_1(t, \xi) \\ \hat{v}_1(t, \xi) \\ \hat{w}_2(t, \xi) \\ \hat{v}_2(t, \xi) \end{pmatrix} d\xi \end{aligned} \quad (1.88)$$

We can show that transformation (1.88) is invertible following the arguments we have used to show the invertibility of the transformation(1.61). The inverse transformation (useful to design our event-triggered controller) is given by

$$\begin{aligned} \begin{pmatrix} \hat{w}_1(t, x) \\ \hat{v}_1(t, x) \\ \hat{w}_2(t, x) \\ \hat{v}_2(t, x) \end{pmatrix} &:= \left(\mathcal{L} \begin{pmatrix} \hat{\alpha}_1(t, \cdot) \\ \hat{\beta}_1(t, \cdot) \\ \hat{\alpha}_2(t, \cdot) \\ \hat{\beta}_2(t, \cdot) \end{pmatrix} \right) (x) \\ &= \begin{pmatrix} \hat{\alpha}_1(t, \cdot) \\ \hat{\beta}_1(t, \cdot) \\ \hat{\alpha}_2(t, \cdot) \\ \hat{\beta}_2(t, \cdot) \end{pmatrix} + \int_0^L \begin{pmatrix} 0 & L_1^{\beta\alpha}(x, \xi) \mathbb{1}_{[0, x]}(\xi) & 0 & 0 \\ 0 & L_1^{\beta\beta}(x, \xi) \mathbb{1}_{[0, x]}(\xi) & 0 & 0 \\ 0 & L^\alpha(x, \xi) & 0 & L_2^{\beta\alpha}(x, \xi) \mathbb{1}_{[x, L]}(\xi) \\ 0 & L^\beta(x, \xi) & 0 & L_2^{\beta\beta}(x, \xi) \mathbb{1}_{[x, L]}(\xi) \end{pmatrix}^T \begin{pmatrix} \hat{\alpha}_1(t, \xi) \\ \hat{\beta}_1(t, \xi) \\ \hat{\alpha}_2(t, \xi) \\ \hat{\beta}_2(t, \xi) \end{pmatrix} d\xi, \end{aligned} \quad (1.89)$$

where the different kernels are bounded functions defined on $\bar{\mathcal{T}}_1$ (kernels L_2^{\cdot}), $\bar{\mathcal{T}}_2$ (kernels L_1^{\cdot}) or $\bar{\mathcal{T}}_3$ (kernels L^{\cdot}). They satisfy the following set of equations on their respective domain of definition

$$(\gamma_i p_i^* - v_i^*) \partial_x L_i^{\beta\alpha}(x, \xi) - v_i^* \partial_\xi L_i^{\beta\alpha}(x, \xi) = 0 \quad (1.90)$$

$$\partial_x L_i^{\beta\beta}(x, \xi) + \partial_\xi L_i^{\beta\beta}(x, \xi) = 0 \quad (1.91)$$

$$(\gamma_1 p_1^* - v_1^*) \partial_x L^\beta(x, \xi) - (\gamma_2 p_2^* - v_2^*) \partial_\xi L^\beta(x, \xi) = 0 \quad (1.92)$$

$$(\gamma_1 p_1^* - v_1^*) \partial_x L^\alpha(x, \xi) + v_2^* \partial_\xi L^\alpha(x, \xi) = 0, \quad (1.93)$$

with the boundary conditions

$$L_i^{\beta\alpha}(x, x) = -\frac{c_i(x)}{\gamma_i p_i^*}, L_1^{\beta\beta}(x, 0) = \frac{v_2^*}{v_1^*} \delta L^\beta(x, 0), \quad (1.94)$$

$$L^\beta(0, \xi) = \frac{r_1}{\delta r_2} L_2^{\beta\beta}(0, \xi), L^\alpha(0, \xi) = \frac{r_1}{\delta r_2} L_2^{\beta\alpha}(0, \xi) \quad (1.95)$$

$$L_2^{\beta\beta}(x, L) = -\exp\left(\frac{-L}{\tau_2 v_2^*}\right) L_2^{\beta\alpha}(x, L), \quad (1.96)$$

$$L^\beta(x, L) = -\exp\left(\frac{-L}{\tau_2 v_2^*}\right) L^\alpha(x, L), \quad (1.97)$$

$$L^\alpha(x, 0) = -(1 - \delta) L^\beta(x, 0) + \frac{v_1^*}{v_2^*} L_1^{\beta\alpha}(x, 0). \quad (1.98)$$

1.3.3 Emulation of the output control law

As aforementioned, we now want to hold the nominal control $U_{\text{nom}}(t)$ constant between two consecutive triggering times. Thus, the emulated version is given as $U_{\text{nom}}(t_k) = U_{\text{nom}}(t) + d(t)$, for all $t \in [t_k, t_{k+1})$. Notice that the output feedback affects the boundary condition (1.40) and (1.29) when introducing what we call “deviation of actuation” $d(t)$. Since we need to assess the impact of the deviation $d(t)$ to the closed-loop system under the event-triggered implementation, we use transformations (1.88) and (1.98) so that we can work on a suitable target system exhibiting the deviation $d(t)$ at the boundary, and from which, we can perform an easier Lyapunov stability analysis. Let us first apply the backstepping transformation (1.88) on the observer system (1.35)-(1.42) and compute the corresponding target system. After straightforward computations, we obtain

$$\partial_t \hat{\alpha}_1(t, x) + v_1^* \partial_x \hat{\alpha}_1(t, x) = p_{\mu_1}(x) \tilde{\alpha}_1(t, L) \quad (1.99)$$

$$\partial_t \hat{\beta}_1(t, x) - (\gamma_1 p_1^* - v_1^*) \partial_x \hat{\beta}_1(t, x) = p_{v_1}(x) \tilde{\alpha}_1(t, L), \quad (1.100)$$

$$\partial_t \hat{\alpha}_2(t, x) - v_2^* \partial_x \hat{\alpha}_2(t, x) = p_{\mu_2}(x) \tilde{\alpha}_1(t, L) \quad (1.101)$$

$$\partial_t \hat{\beta}_2(t, x) + (\gamma_2 p_2^* - v_2^*) \partial_x \hat{\beta}_2(t, x) = p_{v_2}(x) \tilde{\alpha}_1(t, L), \quad (1.102)$$

$$\hat{\alpha}_1(t, 0) = \hat{\alpha}_2(t, 0), \quad (1.103)$$

$$\hat{\beta}_1(t, L) = r_1 \exp\left(\frac{-L}{\tau_1 v_1^*}\right) \hat{\alpha}_1(t, L) + \frac{1-r_1}{\rho_1^*} d, \quad (1.104)$$

$$\hat{\alpha}_2(t, L) \exp\left(\frac{-L}{\tau_2 v_2^*}\right) \frac{1}{r_2} \hat{\beta}_2(t, L), \quad (1.105)$$

$$\hat{\beta}_2(t, 0) = \delta \frac{r_2}{r_1} \hat{\beta}_1(t, 0) + (1 - \delta) r_2 \hat{\alpha}_2(t, 0), \quad (1.106)$$

where

$$p_{\mu_1}(x) = -\mu_1(x), \quad (1.107)$$

$$p_{v_1}(x) = -v_1(x) + \int_0^x K_1^{vw}(x, \xi) \mu_1(\xi) + K_1^{vv}(x, \xi) v_1(\xi) d\xi, \\ + \int_0^L \bar{K}^w(x, \xi) \mu_2(\xi) + K^v(x, \xi) v_2(\xi) d\xi, \quad (1.108)$$

$$p_{\mu_2}(x) = -\mu_2(x), \quad (1.109)$$

$$p_{v_2}(x) = -v_2(x) + \int_x^L K_2^{vw}(x, \xi) \mu_2(\xi) + K_2^{vv}(x, \xi) v_2(\xi) d\xi, \quad (1.110)$$

Note that the functions p_{v_1} and p_{v_2} are well-defined since they are solutions of Volterra equations [16]. Using the inverse transformation (1.89), we can now rewrite the nominal control law U_{nom} defined by (1.78) as a function of the states $\hat{\alpha}_i$ and $\hat{\beta}_i$

$$U_{\text{nom}}(t) = \frac{\rho_1^*}{1-r_1} \left(\int_0^L (L_1^{\beta\alpha}(L, \xi) L_1^{\beta\beta}(L, \xi) L^\alpha(L, \xi) L^\beta(L, \xi)) \begin{pmatrix} \hat{\alpha}_1(t, \xi) \\ \hat{\beta}_1(t, \xi) \\ \hat{\alpha}_2(t, \xi) \\ \hat{\beta}_2(t, \xi) \end{pmatrix} d\xi \right) \quad (1.111)$$

an the corresponding emulated version

$$U_{\text{nom}}(t_k) = \frac{\rho_1^*}{1-r_1} \left(\int_0^L (L_1^{\beta\alpha}(L, \xi) L_1^{\beta\beta}(L, \xi) L^\alpha(L, \xi) L^\beta(L, \xi)) \begin{pmatrix} \hat{\alpha}_1(t_k, \xi) \\ \hat{\beta}_1(t_k, \xi) \\ \hat{\alpha}_2(t_k, \xi) \\ \hat{\beta}_2(t_k, \xi) \end{pmatrix} d\xi \right) \quad (1.112)$$

for all $t \in [t_k, t_{k+1})$. We recall that $U_{\text{nom}}(t_k) = U_{\text{nom}}(t) + d(t)$ where d is given by

$$d(t) = \frac{\rho_1^*}{1-r_1} \left(\int_0^L (L_1^{\beta\alpha}(L,\xi) L_1^{\beta\beta}(L,\xi) L^\alpha(L,\xi) L^\beta(L,\xi)) \begin{pmatrix} \hat{\alpha}_1(t_k,\xi) - \hat{\alpha}_1(t,\xi) \\ \hat{\beta}_1(t_k,\xi) - \hat{\beta}_1(t,\xi) \\ \hat{\alpha}_2(t_k,\xi) - \hat{\alpha}_2(t,\xi) \\ \hat{\beta}_2(t_k,\xi) - \hat{\beta}_2(t,\xi) \end{pmatrix} d\xi \right) \quad (1.113)$$

The function d (which will be fully characterized along with $(t_k)_{k \in \mathbb{N}}$ in the next section) can be viewed as an actuation deviation between the continuous controller and the event-triggered one. Notice that the nominal control, as well as its emulated version are expressed in terms of the kernels of transformation (1.89) and the states of the new target system (1.99)-(1.110). One of the main advantages of such an expression is that it can be easier to work with the target system (particularly when considering the input-to-state stability ISS properties of the system with respect to the deviation d) as well as an easier study of the *growth-in-time* of the deviation of actuation $d(t)$ (which is crucial to prove the avoidance of the so-called Zeno phenomenon). This is of specific interest when emulating the control law and finding conditions that guarantee the closed-loop stability under any event-triggered strategy. This methodology has been used in e.g. [6, 5, 7].

1.4 Observer-based event-triggered boundary control strategy

In this section we study the observer-based event-triggered boundary control strategy proposed in this chapter. It encloses an event-trigger mechanism containing a suitable triggering condition (which determines the time instant at which the controller needs to be updated) and the output backstepping feedback controller (1.112). Before we proceed with the definition of the observer-based event-triggered control, we rewrite first the target systems (1.62)-(1.67) and (1.99)-(1.106) in the following compact forms:

$$\partial_t \tilde{y}(t, x) + \Lambda \partial_x \tilde{y}(t, x) = 0, \quad (1.114)$$

$$\partial_t \hat{y}(t, x) + \Lambda \partial_x \hat{y}(t, x) = F(x) \tilde{\alpha}_1(t, L), \quad t \in \mathbb{R}^+, x \in [0, 1] \quad (1.115)$$

where $\Lambda = \text{diag}(\Lambda^+, -\Lambda^-)$ with

$$\Lambda^+ = \text{diag}(v_1^*, (\gamma_2 p_2^* - v_2^*)), \quad \Lambda^- = \text{diag}((\gamma_1 p_1^* - v_1^*), v_2^*), \quad (1.116)$$

and $F(x) = (p_{\mu_1}(x), p_{v_2}(x), p_{v_1}(x), p_{\mu_2}(x))^T$. We use the notation $\tilde{y} := \begin{pmatrix} \tilde{y}^+ \\ \tilde{y}^- \end{pmatrix}$ with $\tilde{y}^+ := \begin{pmatrix} \tilde{\alpha}_1 \\ \tilde{\beta}_2 \end{pmatrix}$, $\tilde{y}^- := \begin{pmatrix} \tilde{\beta}_1 \\ \tilde{\alpha}_2 \end{pmatrix}$ and $\hat{y} := \begin{pmatrix} \hat{y}^+ \\ \hat{y}^- \end{pmatrix}$ with $\hat{y}^+ := \begin{pmatrix} \hat{\alpha}_1 \\ \hat{\beta}_2 \end{pmatrix}$, $\hat{y}^- := \begin{pmatrix} \hat{\beta}_1 \\ \hat{\alpha}_2 \end{pmatrix}$. In addition, the boundary conditions can be rewritten as

$$\begin{pmatrix} \tilde{y}^+(t,0) \\ \tilde{y}^-(t,L) \end{pmatrix} = G \begin{pmatrix} \tilde{y}^+(t,L) \\ \tilde{y}^-(t,0) \end{pmatrix}, \quad \begin{pmatrix} \hat{y}^+(t,0) \\ \hat{y}^-(t,L) \end{pmatrix} = G \begin{pmatrix} \hat{y}^+(t,L) \\ \hat{y}^-(t,0) \end{pmatrix} + Bd(t), \quad (1.117)$$

where $B = \left(0, 0, \frac{1-r_1}{\rho_1^*}, 0\right)^\top$, $G := \begin{pmatrix} 0_{2,2} & G^+ \\ G^- & 0_{2,2} \end{pmatrix}$ with $G^+ = \begin{pmatrix} 0 & 1 \\ \delta \frac{r_2}{r_1} & (1-\delta)r_2 \end{pmatrix}$ and $G^- = \begin{pmatrix} r_1 \exp\left(\frac{-L}{\tau_1 v_1^*}\right) & 0 \\ 0 & \frac{1}{r_2} \exp\left(\frac{-L}{\tau_2 v_2^*}\right) \end{pmatrix}$.

In addition, using the solutions to (1.94)-(1.98) along with (1.107)-(1.110), we introduce the following variables:

$$\kappa_{\hat{\alpha}_1} := \frac{\rho_1^*}{1-r_1} \left(v_1^* L_1^{\beta\alpha}(L, L) - (\gamma_1 p_1^* - v_1^*) r_1 \exp\left(\frac{-L}{\tau_1 v_1^*}\right) L_1^{\beta\beta}(L, L) \right), \quad (1.118)$$

$$\kappa_{\hat{\beta}_1} := \frac{\rho_1^*}{1-r_1} \left((\gamma_1 p_1^* - v_1^*) L_1^{\beta\beta}(L, 0) - (\gamma_2 p_2^* - v_2^*) \delta \frac{r_2}{r_1} L^\beta(L, 0) \right), \quad (1.119)$$

$$\begin{aligned} \kappa_{\hat{\alpha}_2} &:= \frac{\rho_1^*}{1-r_1} \left(-v_1^* L_1^{\beta\alpha}(L, 0) + v_2^* L^\alpha(L, 0) \right. \\ &\quad \left. - (\gamma_2 p_2^* - v_2^*) (1-\delta) r_2 L^\beta(L, 0) \right), \end{aligned} \quad (1.120)$$

$$\kappa_{\hat{\beta}_2} := \frac{\rho_1^*}{1-r_1} \left(-v_2^* \frac{1}{r_2} \exp\left(\frac{-L}{\tau_2 v_2^*}\right) L^\alpha(L, L) + (\gamma_2 p_2^* - v_2^*) L^\beta(L, L) \right), \quad (1.121)$$

$$\begin{aligned} \kappa_{\tilde{\alpha}_1} &:= \frac{\rho_1^*}{1-r_1} \left(\int_0^L \begin{pmatrix} L_1^{\beta\alpha}(L, \xi) & L_1^{\beta\beta}(L, \xi) & L^\alpha(L, \xi) & L^\beta(L, \xi) \end{pmatrix} \right. \\ &\quad \left. \cdot \begin{pmatrix} p_{\mu_1}(x) \\ p_{v_1}(x) \\ p_{\mu_2}(x) \\ p_{v_2}(x) \end{pmatrix} d\xi \right), \end{aligned} \quad (1.122)$$

$$\begin{aligned} \varepsilon_0 &:= 2 \left(\frac{\rho_1^*}{1-r_1} \right)^2 \max \left\{ \int_0^L \left(v_1^* \partial_\xi L_1^{\beta\alpha}(L, \xi) \right)^2, \int_0^L \left((\gamma_1 p_1^* - v_1^*) \partial_\xi L_1^{\beta\beta}(L, \xi) \right)^2, \right. \\ &\quad \left. \int_0^L \left(v_2^* \partial_\xi L^\alpha(L, \xi) \right)^2 d\xi, \int_0^L \left((\gamma_2 p_2^* - v_2^*) \partial_\xi L^\beta(L, \xi) \right)^2 d\xi \right\}, \end{aligned} \quad (1.123)$$

$$\varepsilon_1 := 4 \left((\gamma_1 p_1^* - v_1^*) L_1^{\beta\beta}(L, L) \right)^2, \quad (1.124)$$

$$\varepsilon_2 := 4 \kappa_{\tilde{\alpha}_1}^2 \quad (1.125)$$

$$\mathcal{D}_0 := \text{diag} \left(8 \kappa_{\tilde{\alpha}_1}^2, 8 \kappa_{\hat{\beta}_2}^2, 8 \kappa_{\hat{\beta}_1}^2, 8 \kappa_{\hat{\alpha}_2}^2 \right). \quad (1.126)$$

1.4.1 Definition of observer-based event-triggered boundary controller

The event-triggering condition is based on the evolution of the square of the actuation deviation (1.113) and of a dynamic variable satisfying a suitable ODE. It relies, in turn, on a Lyapunov function candidate for the target systems (1.114)-(1.115) that we define as follows (see [4, Section 5], [15],[13]):

$$V(\tilde{y}, \hat{y}) := V_1(\tilde{y}) + CV_2(\hat{y}) = \int_0^L \tilde{y}^\top(x) \mathbf{Q}(x) \tilde{y}(x) dx + C \int_0^L \hat{y}^\top(x) \mathbf{Q}(x) \hat{y}(x) dx, \quad (1.127)$$

where $\mathbf{Q}(x) = \text{diag}[\mathbf{Q}^+(x), \mathbf{Q}^-(x)] = \text{diag}[e^{-\mu x} \mathbf{Q}^+, e^{\mu x} \mathbf{Q}^-]$ with $\mu > 0$, $C > 0$, and diagonal positive definite matrices $\mathbf{Q}^- \in \mathbb{R}^{2 \times 2}$ and $\mathbf{Q}^+ \in \mathbb{R}^{2 \times 2}$ and such that $\mathbf{Q}(x)\Lambda = \Lambda \mathbf{Q}(x)$. Moreover, we use the fact that there exist $\underline{\varrho}$, $\bar{\varrho}$ (depending on the eigenvalues of \mathbf{Q}^+ , \mathbf{Q}^- and on μ) such that $\underline{\varrho} \|\hat{y}(t, \cdot)\|_{L^2}^2 \leq V_2(\hat{y}(t, \cdot)) \leq \bar{\varrho} \|\hat{y}(t, \cdot)\|_{L^2}^2$.

Definition 1 Let $\theta_0, \theta_1 > 0$, $\eta > 0$, $\nu > 0$, $\sigma \in (0, 1)$. Let ε_2 and \mathcal{D}_0 be given by (1.125) and (1.126), respectively. Let $t \mapsto V(\tilde{y}(t, \cdot), \hat{y}(t, \cdot))$ be given by (1.127) with diagonal positive definite matrices $\mathbf{Q}^- \in \mathbb{R}^{2 \times 2}$ and $\mathbf{Q}^+ \in \mathbb{R}^{2 \times 2}$ and $C > 0$. The observer-based event-triggered boundary control is defined by considering the following components:

I) (The event-trigger) The times of the events $t_k \geq 0$ with $t_0 = 0$ form a finite or countable set of times which is determined by the following rules for some $k \geq 0$:

- a) if $\{t \in \mathbb{R}^+ | t > t_k \wedge \theta_1 C \left(\frac{1-r_1}{\rho_1^*}\right)^2 d^2(t) \geq \frac{\nu}{2} \sigma V(t) - \frac{1}{\theta_0} m(t)\} = \emptyset$ then the set of the times of the events is $\{t_0, \dots, t_k\}$.
- b) if $\{t \in \mathbb{R}^+ | t > t_k \wedge \theta_1 C \left(\frac{1-r_1}{\rho_1^*}\right)^2 d^2(t) \geq \frac{\nu}{2} \sigma V(t) - \frac{1}{\theta_0} m(t)\} \neq \emptyset$, then the next event time is given by:

$$t_{k+1} = \inf\{t \in \mathbb{R}^+ | t > t_k \wedge \theta_1 C \left(\frac{1-r_1}{\rho_1^*}\right)^2 d^2(t) \geq \frac{\nu}{2} \sigma V(t) - \frac{1}{\theta_0} m(t)\}. \quad (1.128)$$

where the actuation deviation $d(t)$ is given by (1.113) for all $t \in [t_k, t_{k+1})$, and m satisfies the ordinary differential equation,

$$\begin{aligned} \dot{m}(t) = & -\eta m(t) + \left(\theta_1 C \left(\frac{1-r_1}{\rho_1^*}\right)^2 d^2(t) - \frac{\nu}{2} \sigma V(t) \right. \\ & \left. - 2\theta_0 \theta_1 C \left(\frac{1-r_1}{\rho_1^*}\right)^2 \left(\begin{pmatrix} \hat{y}^+(t, L) \\ \hat{y}^-(t, 0) \end{pmatrix}^\top \mathcal{D}_0 \begin{pmatrix} \hat{y}^+(t, L) \\ \hat{y}^-(t, 0) \end{pmatrix} + \varepsilon_2 \tilde{\alpha}^2(t, L) \right) \right), \end{aligned} \quad (1.129)$$

for all $t \in (t_k, t_{k+1})$ with $\eta \geq \frac{\nu}{2}(1 - \sigma)$, $m(0) = m^0 < 0$, and $m(t_k^-) = m(t_k) = m(t_k^+)$.

II) (the control action) The output boundary feedback law is defined by

$$U_{\text{nom}}(t_k) = \frac{\rho_1^*}{1-r_1} \left(\int_0^L \begin{pmatrix} L_1^{\beta\alpha}(L,\xi) & L_1^{\beta\beta}(L,\xi) & L^\alpha(L,\xi) & L^\beta(L,\xi) \end{pmatrix} \begin{pmatrix} \tilde{\alpha}_1(t_k,\xi) \\ \tilde{\beta}_1(t_k,\xi) \\ \tilde{\alpha}_2(t_k,\xi) \\ \tilde{\beta}_2(t_k,\xi) \end{pmatrix} d\xi \right), \quad (1.130)$$

for all $t \in [t_k, t_{k+1})$.

Remark 1 Although the function $V(t)$ and the function $m(t)$ depend on $\tilde{\alpha}_i(t, \cdot)$ and $\tilde{\beta}_i(t, \cdot)$ (which are a priori unknown), this is not a problem as these functions can be expressed as delayed functions of the measurement $y(t)$ and of the observer state. Indeed, we have $\tilde{\alpha}(t, L) = \tilde{w}(t, L) = y(t) - \hat{w}(t, L)$, which means that the function $\tilde{\alpha}(t, 1)$ can be computed from the measurement. From (1.62)-(1.67), we immediately have for all $x \in [0, 1]$

$$\beta_1(t, x) = r_1 \exp\left(\frac{-L}{\tau_1 v_1^*}\right) \tilde{\alpha}_1\left(t - \frac{(L-x)}{\gamma_1 p_1^* - v_1^*}, L\right), \quad (1.131)$$

which means that we can also compute the function $\beta_1(t, x)$ from the measurement. Consider now the function $\alpha_2(t, 0)$. We have (using the method of characteristics)

$$\begin{aligned} \tilde{\alpha}_2(t, 0) &= \exp\left(\frac{-L}{\tau_2 v_2^*}\right) (1-\delta) \tilde{\alpha}_2\left(t - \frac{1}{v_2^*} - \frac{1}{\gamma_2 p_2^* - v_2^*}, 0\right) \\ &\quad + \frac{\delta}{r_1} \exp\left(\frac{-L}{\tau_2 v_2^*}\right) \tilde{\beta}_1\left(t - \frac{1}{v_2^*} - \frac{1}{\gamma_2 p_2^* - v_2^*}, 0\right). \end{aligned} \quad (1.132)$$

Applying the method of characteristics on the term $\alpha_2(t, 0)$ that appear on the right side of the above equation, and iterating N times the procedure, we obtain

$$\begin{aligned} \tilde{\alpha}_2(t, 0) &= \left(\exp\left(\frac{-L}{\tau_2 v_2^*}\right) (1-\delta)\right)^N \tilde{\alpha}_2\left(t - N\left(\frac{1}{v_2^*} + \frac{1}{\gamma_2 p_2^* - v_2^*}\right), 0\right) \\ &\quad + F(\tilde{\beta}_1(t, 0)), \end{aligned} \quad (1.133)$$

where the function F only depends on delayed values of $F(\tilde{\beta}_1(t, 0))$. Choosing N such that $N\left(\frac{1}{v_2^*} + \frac{1}{\gamma_2 p_2^* - v_2^*}\right) - \frac{1}{v_1^*}$ and using equation (1.64), we obtain

$$\begin{aligned} \tilde{\alpha}_2(t, 0) &= \left(\exp\left(\frac{-L}{\tau_2 v_2^*}\right) (1-\delta)\right)^N \tilde{\alpha}_1\left(t - N\left(\frac{1}{v_2^*} + \frac{1}{\gamma_2 p_2^* - v_2^*}\right) + \frac{1}{v_1^*}, L\right) \\ &\quad + F(\tilde{\beta}_1(t, 0)). \end{aligned} \quad (1.134)$$

Thus, we can compute the function $\tilde{\alpha}_2(t, 0)$ using the available measurement. Using the method of the characteristics, it becomes straightforward to express $\tilde{\alpha}_i(t, x)$ and $\tilde{\beta}_i(t, x)$ as delayed functions of the available measurements.

Consequently, the proposed event-triggered strategy is implementable simply using the available measurement (and the observer state).

We directly have the following lemma.

Lemma 1 *Under the definition of the observer-based event triggered boundary control (1.130) with the dynamic trigger condition (1.128), it holds that $\theta_1 C \left(\frac{1-r_1}{\rho_1^*} \right)^2 d^2(t) - \frac{\nu}{2} \sigma V(t) + m(t) < 0$ and $m(t) < 0$ for $t \in [0, T)$ where $T = \lim_{k \rightarrow \infty} (t_k)$.*

Proof The proof follows the same lines of [6, Lemma 1].

The following result is useful to analyze the growth-in-time of the actuation deviation. A suitable characterization is given in the following lemma which is instrumental to derive the existence of a minimal dwell-time.

Lemma 2 *For $d(t)$ given by (1.113), it holds for all $t \in (t_k, t_{k+1})$,*

$$(\dot{d}(t))^2 \leq \varepsilon_0 \frac{1}{\underline{\rho} C} V(t) + \varepsilon_1 d^2(t) + \varepsilon_2 \tilde{\alpha}^2(t, L) + \begin{pmatrix} \hat{y}^+(t, L) \\ \hat{y}^-(t, 0) \end{pmatrix}^\top \mathcal{D}_0 \begin{pmatrix} \hat{y}^+(t, L) \\ \hat{y}^-(t, 0) \end{pmatrix}, \quad (1.135)$$

for some $\underline{\rho} > 0$, and with ε_0 , ε_1 , ε_2 and \mathcal{D}_0 given by (1.123), (1.124), (1.125) and (1.126), respectively.

Proof The proof follows the same lines of [6, Lemma 2].

1.5 Main results

In this section we present our main results: the avoidance of the Zeno phenomenon and the exponential convergence in L^2 -norm of the closed-loop system.

1.5.1 Avoidance of the Zeno phenomenon

We first prove the avoidance of the Zeno phenomenon.

Theorem 1 *Under the event-triggered boundary control (1.130)-(1.128) in Definition 1, with parameters satisfying*

$$\theta_0 \theta_1 < \underline{\rho} \left(\frac{\rho_1^*}{1-r_1} \right)^2 \frac{\nu \sigma}{4\varepsilon_0}, \quad (1.136)$$

there exists a minimal dwell-time $\tau^* > 0$ between two triggering times, i.e. there exists a constant $\tau^* > 0$ (independent of the initial conditions) such that $t_{k+1} - t_k \geq \tau^*$, for all $k \geq 0$. Moreover, τ^* can be given by

$$\tau^* = \int_0^1 \frac{1}{a_0 + a_1 s + a_2 s^2} ds, \quad (1.137)$$

with $a_0 = 1 + \varepsilon_1 + \frac{1}{2\theta_0} + \eta$, $a_1 = 1 + \varepsilon_1 + \frac{1}{2\theta_0} + \eta$ and $a_2 = \frac{1}{2\theta_0}$.

Proof It follows the methodology employed in [6, 5] and makes uses of estimate (1.135) in Lemma 2.

Remark 2 Since there is a minimal dwell-time (which is uniform and does not depend on initial conditions), no Zeno solution can appear. This has a very important consequence as it allows to guarantee the existence and uniqueness of the closed-loop solution. The solution, can be constructed by the step method. We omit the details of well-posedness in this chapter, but we refer to [5, 13] for further details on the notion of the considered solutions.

1.5.2 Lyapunov-based analysis

We perform a Lyapunov-based analysis on the target systems written in compact form i.e. (1.114)-(1.115) and we take into account the proposed event-triggered control strategy (1.128)- (1.130). In what follows, we define the following variables

$$\bar{\mathcal{D}}_0 = 2\theta_0\theta_1 \left(\frac{1-r_1}{\rho_1^*} \right)^2 \mathcal{D}_0, \quad (1.138)$$

with \mathcal{D}_0 given by (1.126);

$$\mathcal{D}_1 = \begin{pmatrix} \mathbf{Q}^+(0)\Lambda^+ & 0_{2,2} \\ 0_{2,2} & \mathbf{Q}^-(L)\Lambda^- \end{pmatrix}, \quad (1.139)$$

$$\mathcal{D}_2 = \begin{pmatrix} \mathbf{Q}^+(L)\Lambda^+ & 0_{2,2} \\ 0_{2,2} & \mathbf{Q}^-(0)\Lambda^- \end{pmatrix}, \quad (1.140)$$

for $\mathbf{Q}(x)$ as in (1.127), and

$$\mathcal{D}_3 = \begin{pmatrix} \frac{\theta_2}{2} + 2\theta_0\theta_1 C \left(\frac{1-r_1}{\rho_1^*} \right)^2 \varepsilon_2 & 0_{1,3} \\ 0_{3,1} & 0_{3,3} \end{pmatrix}, \quad (1.141)$$

with some $\theta_2 > 0$. The notation $0_{i,j}$ stands for the matrix with i rows and j columns whose all components are zero.

Theorem 2 Let $\theta_0 > 0$, $\sigma \in (0,1)$, ε_0 , ε_2 be given by (1.123), (1.125), respectively and \mathcal{D}_0 be given by (1.138). Let \mathcal{D}_1 , \mathcal{D}_2 and \mathcal{D}_3 be given by (1.139),(1.140) and (1.141), respectively. Let (1.136) hold. If there exist $\theta_1, \theta_2 > 0$, $\mu > 0$, $\nu > 0$ (thus there exists $\eta \geq \frac{\nu}{2}(1 - \sigma)$) and diagonal positive definite matrices $\mathbf{Q}^- \in \mathbb{R}^{2 \times 2}$ and $\mathbf{Q}^+ \in \mathbb{R}^{2 \times 2}$ such that for $\mathbf{Q}(x)$ given in (1.127) the following conditions hold,

$$G^\top \mathcal{D}_1 G - \mathcal{D}_2 + \mathcal{D}_3 < 0, \quad (1.142)$$

$$\begin{pmatrix} \bar{\mathcal{D}}_0 + G^\top \mathcal{D}_1 G - \mathcal{D}_2 & G^\top \mathcal{D}_1 \\ (G^\top \mathcal{D}_1)^\top & \mathcal{D}_1 - \theta_1 I_{4,4} \end{pmatrix} < 0, \quad (1.143)$$

then, the closed-loop system (1.24)-(1.31) with event-triggered control (1.130), (1.128) is exponentially convergent in the L^2 -norm.

Proof It follows by considering the following Lyapunov function candidate for the target systems (1.114)-(1.115) along with (1.129), defined for all $\tilde{y} \in L^2((0, L); \mathbb{R}^4)$, $\hat{y} \in L^2((0, L); \mathbb{R}^4)$ and $m \in \mathbb{R}^-$ by

$$W(\tilde{y}, \hat{y}, m) := V(\tilde{y}, \hat{y}) - m \quad (1.144)$$

and establishing that the time derivative of (1.144) along the solutions is upper estimated (after using the sufficient conditions (1.142)-(1.143) and Lemma 1) as follows:

$$\dot{W}(t) \leq -\frac{\nu}{2}(1 - \sigma)W(t). \quad (1.145)$$

Using the comparison principle and the bounded invertibility of the backstepping transformations we obtain the exponential convergence in the L^2 -norm.

Remark 3 In Theorem 2, we have established the exponential convergence of the closed-loop system to the equilibrium point. We could have obtained exponential stability if we set $m^0 = 0$. However, if $m^0 = 0$, then $m(t) \leq 0$. This specific issue may affect the conclusion on the existence of a minimal-dwell as stated in Theorem 1. Hence, we opted to choose m^0 strictly negative.

1.6 Numerical simulations

The length of each freeway segment is chosen to be $L = 1$ km so the total length of the two connected segments are 2 km. The simulation time is $T = 16$ min. The maximum speed limit is $v_m = 40$ m/s = 144 km/h. We consider 6 lanes for the downstream freeway segment 1. Assuming the average vehicle length is 5 m plus the minimum safety distance of 50% vehicle length, the maximum density of the road is obtained as $\rho_{m,1} = 6/7.5$ vehicles/m = 800 vehicles/km. The upstream segment has less functional lanes thus its maximum density is $\rho_{m,2} = 700$ vehicles/km. We take $\gamma_i = 0.5$. The steady states (ρ_1^*, v_1^*) and (ρ_2^*, v_2^*) are chosen respectively as (600 vehicles/km, 19.4 km/h) and (488.6 vehicles/km, 23.8 km/h), both of which are in the congested regime. The constant flow rate is $q^* = \rho_1^* v_1^* = \rho_2^* v_2^* = 11640$ vehicles/h, same for the two segments. If we consider the segment 1 with 6 lanes, then the averaged flow rate of each lane is 1940 vehicles/h/lane. The equilibrium steady state of the downstream road

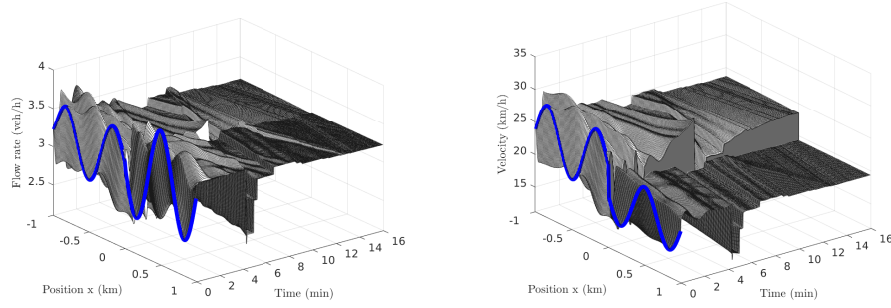


Fig. 1.3 Numerical solution of the flow rate and velocity with the ramp meeting event-triggered output control $U_{\text{nom}}(t_k)$ which is updated according to the observer-based event-triggered output control (1.128) .

has higher density and lower velocity, thus is more congested than the upstream road. The relaxation time is $\tau_1 = 90$ s and $\tau_2 = 60$ s. We use sinusoid initial conditions for flow rate and velocity field which represent the initial stop-and-go oscillations on the connected freeway. We perform the simulation on a time horizon of 16 min.

Event-triggered implementation and closed-loop simulation

The parameters involved in the observer-based event-triggering boundary controller are $r_1 = -0.44$, $r_2 = -0.64$, $\varepsilon_0 = 6.4 \times 10^{-3}$, $\varepsilon_1 = 4.08 \times 10^{-3}$, $\varepsilon_2 = 1.73 \times 10^3$, $\kappa_{\hat{\alpha}_1} = 0.41$, $\kappa_{\hat{\beta}_1} = 3.45$, $\kappa_{\hat{\alpha}_2} = -1.45$, $\kappa_{\hat{\beta}_2} = -0.94$, $\kappa_{\hat{\alpha}_1} = 22.19$. Then, we select $\theta_0 = 500$, $\sigma = 0.09$. Moreover, we perform a line search on μ while finding θ_1 , θ_2 , Q^+ and Q^- must verify conditions (1.136), (1.142) and (1.143) (using e.g. semi-definite programming combined with line search algorithm). We obtain $\mu = 1.01$, $\theta_1 = 0.061$, $\theta_2 = 1.3 \times 10^{-3}$, $Q^+ = \begin{pmatrix} 0.835 & 0 \\ 0 & 0.476 \end{pmatrix}$, $Q^- = \begin{pmatrix} 1.58 & 0 \\ 0 & 1.80 \end{pmatrix}$. We obtain also $\nu = 5.4 \times 10^{-3}$, $\eta = 0.0493$, $C = 1.76 \times 10^{-4}$. Hence, Theorem 2 applies. Moreover, we compute the minimal dwell-time between two triggering times according to (1.137), that is $\tau^* = 0.65$. We stabilize the system on events under the event-triggered boundary control (1.130), (1.128). Figure 1.3 shows the numerical solution of flow rate and velocity with the ramp meeting event-triggered output control $U_{\text{nom}}(t_k)$ which is updated according to the observer-based event-triggered output control (1.128). Figure 1.4 shows the time-evolution of the control signal (recall that designed controller U_{nom} is the flow rate perturbation around a nominal flow rate), where we can observe that the updating is aperiodically, only when needed.

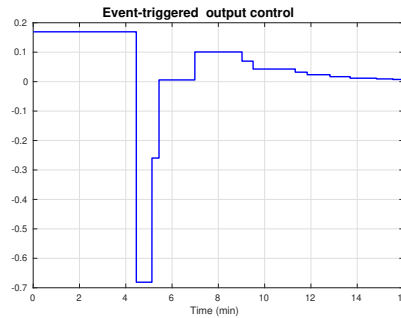


Fig. 1.4 Time-evolution of the event-triggered output control. The updating is aperiodically, according with (1.128).

1.7 Conclusion

In this chapter, we developed an event-triggered boundary output feedback control for simultaneous stabilization of traffic flow on connected roads. We built on the linearized ARZ model and designed a ramp metering strategy as a boundary control, through the backstepping method. The updating of the control signal is done according to a suitable dynamic triggering condition. We proved that under this strategy, there exists a uniform minimal dwell-time (independent of initial conditions), thus avoiding the Zeno phenomenon and we guaranteed the exponential convergence of the closed-loop system under the proposed event-triggered boundary control. Future work includes the design of periodic event-triggered control strategy to monitor the triggering condition periodically, hence, saving computational resources.

References

1. J. Auriol and F. Di Meglio. An explicit mapping from linear first order hyperbolic PDEs to difference systems. *Systems & Control Letter*, 123:144–150, 2019.
2. J. Auriol and F. Di Meglio. Robust output feedback stabilization for two heterodirectional linear coupled hyperbolic PDEs. *Automatica*, 115:108896, 2020.
3. A. Aw and M. Rascole. Resurrection of "second order" models of traffic flow. *SIAM Journal on Applied Mathematics*, 60(3):916–938, 2000.
4. G. Bastin and J.-M. Coron. *Stability and Boundary Stabilization of 1-D Hyperbolic Systems*. Birkhäuser Basel, 2016.
5. N. Espitia. Observer-based event-triggered boundary control of a linear 2×2 hyperbolic systems. *Systems & Control Letters*, 138, 2020.
6. N. Espitia, A. Girard, N. Marchand, and C Prieur. Event-based boundary control of a linear 2×2 hyperbolic system via backstepping approach. *IEEE Transactions on Automatic Control*, 63(8):2686–2693, 2018.
7. N. Espitia, H. Yu, and M. Krstic. Event-triggered varying speed limit control for stop-and-go traffic. In *Proc of the IFAC World Congress*, Berlin, 2020.

8. S. Fan and B. Seibold. Data-fitted first-order traffic models and their second-order generalizations: Comparison by trajectory and sensor data. *Transportation Research Record 2391*, 1:32–43, 2013.
9. M. Garavello and B. Piccoli. Traffic flow on a road network using the aw–rascle model. *Communications in Partial Differential Equations*, 31(2):243–275, 2006.
10. M. Herty and M. Rascle. Coupling conditions for a class of second-order models for traffic flow. *SIAM Journal on mathematical analysis*, 38(2):595–616, 2006.
11. Coron J.-M., L. Hu, and G. Olive. Stabilization and controllability of first-order integro-differential hyperbolic equations. *Journal of Functional Analysis*, 271:554–3587, 2016.
12. I. Karafyllis and M. Papageorgiou. Feedback control of scalar conservation laws with application to density control in freeways by means of variable speed limits. *Automatica*, 105:228–236, 2019.
13. C. Prieur, A. Girard, and E. Witrant. Stability of switched linear hyperbolic systems by Lyapunov techniques. *IEEE Transactions on Automatic Control*, 59(8):2196–2202, 2014.
14. J. Smoller. *Shock waves and reaction—diffusion equations*, volume 258. Springer Science & Business Media, 2012.
15. R. Vazquez, J.-M. Coron, M. Krstic, and G. Bastin. Collocated output-feedback stabilization of a 2×2 quasilinear hyperbolic system using backstepping. In *American Control Conference (ACC), 2012*, pages 2202–2207, Fairmont Queen Elizabeth, Montreal, Canada, 2012.
16. K. Yoshida. *Lectures on differential and integral equations*, volume 10. Interscience Publishers, 1960.
17. H. Yu, J. Auriol, and M. Krstic. Simultaneous downstream and upstream output-feedback stabilization of cascaded freeway traffic. *Under review in Automatica.*, 2021.
18. H. Yu and M. Krstic. Varying speed limit control of Aw-Rascl-Zhang traffic model. In *Proceedings of the 21st International conference on Intelligent Transportation Systems (ITSC)*, pages 1846–1851, Maui, HI, USA, 2018.
19. H. Yu and M. Krstic. Traffic congestion control for Aw-Rascl-Zhang model. *Automatica*, 100:38–51, 2019.
20. H.M. Zhang. A non-equilibrium traffic model devoid of gas-like behavior. *Transportation Research Part B: Methodological*, 36(3):275–290, 2002.
21. L. Zhang, C. Prieur, and J. Qiao. Pi boundary control of linear hyperbolic balance laws with stabilization of arz traffic flow models. *Systems & Control Letters*, 123:85–91, 2019.